

# Sinusoidal phase-modulating Fizeau interferometer using a self-pumped phase conjugator for surface profile measurements

Xiangzhao Wang  
Niigata University  
The Graduate School of Science and  
Technology  
Niigata, Japan 950-21

Osami Sasaki  
Yuuichi Takebayashi  
Takamasa Suzuki  
Takeo Maruyama  
Niigata University  
Faculty of Engineering  
Niigata, Japan 950-21

**Abstract.** A sinusoidal phase-modulating Fizeau interferometer using a BaTiO<sub>3</sub> self-pumped phase conjugator is constructed to measure surface profiles of objects with a high accuracy. An object field is formed on a surface of a glass plate where the object wave interferes with its phase conjugate wave. Because the size of the glass plate can be much smaller than that of the object, the sinusoidal phase modulation by vibrating the glass plate is easy and accurate for measurements of the surface profiles of large-diameter objects. The interferometer is self-referencing and free of the phase fluctuations of the object wave caused by spatially uniform movements of objects. The usefulness of the interferometer is made clear through the surface profile measurements of a diamond-turned aluminum disk and mirror.

*Subject terms: surface profile measurement; interferometry; phase conjugation.*  
*Optical Engineering 33(8), 2670–2674 (August 1994).*

## 1 Introduction

Recently, there has been much interest in applications of phase conjugators, especially self-pumped conjugators, to interferometry. Self-pumped conjugators have been applied to Twyman-Green interferometers<sup>1</sup> for testing conicoidal surfaces,<sup>2</sup> analysis of thin films,<sup>3</sup> and testing laser beam collimation<sup>4</sup> and have also been applied to Fizeau interferometers.<sup>5</sup> Among these applications the phase conjugate Fizeau interferometer is very interesting. In this interferometer an incident light wave interferes with its phase conjugate wave generated from a BaTiO<sub>3</sub> self-pumped conjugator to measure a phase distribution of the incident light wave. Therefore, this interferometer does not need another reference wave, that is, the interferometer is self-referencing. This property is very attractive in measuring a phase distribution of the wavefront. However, the interferometer can not be directly applied to measuring surface profiles of objects.

In this paper, we propose a phase conjugate Fizeau interferometer for surface profile measurements of objects. To achieve the measurements, the light reflected by the object is transformed with two lenses to make an object field on a glass plate. The complex amplitude distribution of the field is identical to that of the original object field. The object field is considered as the object wave. The self-pumped phase

conjugate wave of the object field is produced on the glass plate and is considered as the reference wave. The object wave is phase modulated by vibrating the glass plate sinusoidally with piezoelectric transducers (PZTs) to use sinusoidal phase-modulating (SPM) interferometry. The surface profile of the object is obtained with a high accuracy through the signal processing employed in SPM interferometry.<sup>6,7</sup>

The new interferometer for surface profile measurements is based on the combination of the phase conjugate Fizeau interferometer and SPM interferometry, so the interferometer incorporates advantages of both of them. It produces attractive characteristics in the interferometer that both the reference and object waves are generated from the beam reflected by the object. First, the interferometer is completely free of the phase fluctuations of the object wave caused by spatially uniform vibrations of the object because spatially uniform phase changes of the object wave are not reversed on the self-pumped phase conjugation.<sup>8</sup> Next, the measurement sensitivity is twice as high as that of conventional interferometers for surface profile measurements. Finally, because the object wave can be reduced on the glass plate, the dimensions of the glass plate can be much smaller than those of the objects. This feature makes it easy to perform a sinusoidal phase modulation of constant amplitude over the whole glass plate at high frequency and leads the improvement of measurement accuracy in the case of the measurement of large-diameter objects.

We first describe the principle of the new SPM Fizeau interferometer with a self-pumped conjugator for surface pro-

Paper 32103 received Oct. 25, 1993; revised manuscript received Jan. 29, 1994; accepted for publication Jan. 30, 1994.  
© 1994 Society of Photo-Optical Instrumentation Engineers. 0091-3286/94/\$6.00.

file measurements. Next the characteristics of the interferometer are made clear through measurements of the surface profile of a diamond-turned aluminum disk. Finally we modify the configuration of the interferometer to measure the surface profiles of large-diameter objects.

## 2 Principle

### 2.1 Interferometer

Figure 1 shows a SPM Fizeau interferometer using a self-pumped phase conjugator. A laser beam collimated with lenses  $L_1$  and  $L_2$  is employed to illuminate the object through beamsplitter  $BS_1$ . The object field generated by the illumination of the beam can be represented by

$$U_o(x) = \exp[2jkr(x)] \quad (1)$$

where  $r(x)$  is the surface profile of the object,  $x$  is a coordinate on the object, and  $k$  is the wave number. The beam reflected by the object is bent at right angles by beamsplitter  $BS_1$ . Lenses  $L_3$  and  $L_4$  make an object field in the image space at the surface of the glass plate. The beam transmitted through the glass plate is focused with lens  $L_6$  into the self-pumped conjugator of a BaTiO<sub>3</sub> crystal, which produces a phase conjugate wave. The phase conjugate wave interferes with the object wave on the glass plate. In this interferometer, the phase conjugate wave is considered as the reference wave, and the beam reflected by the glass plate is considered as the object wave.

SPM interferometry is used to obtain the phase distribution of the interference pattern. To phase modulate the object wave, the glass plate is sinusoidally vibrated with PZTs. The vibration of the glass plate is expressed by

$$A(t) = a \cos(\omega_c t + \theta) \quad (2)$$

where  $A(t)$  is a glass plate shift in the direction along the incident wave. The reference and object fields on the glass plate can be written as

$$U_{1r}(x') = R \exp[-2jkr(x')] \quad (3)$$

$$U_{1o}(x') = \exp[2jkr(x') + Z \cos(\omega_c t + \theta)] \quad (4)$$

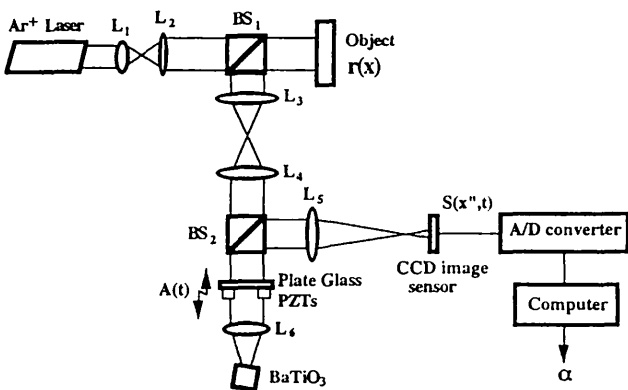


Fig. 1 SPM Fizeau interferometer using a self-pumped phase conjugator.

where  $R$  is the phase-conjugate reflectivity,  $Z = (4\pi/\lambda)a$ ,  $\lambda$  is wavelength, and  $x'$  is a coordinate on the glass plate. Lens  $L_5$  images these fields on a 1-D CCD image sensor. The interference pattern generated from  $U_{1r}(x')$  and  $U_{1o}(x')$  on the CCD image sensor is expressed as

$$I(x'', t) = 1 + R^2 + 2R \cos[Z \cos(\omega_c t + \theta) + \alpha] \quad (5)$$

where

$$\alpha = (8\pi/\lambda)r(x'') \quad (6)$$

and  $x''$  is a coordinate on the CCD image sensor. The ac component of the interference signal,

$$S(x'', t) = S_o \cos[Z \cos(\omega_c t + \theta) + \alpha] \quad (7)$$

is detected with the CCD image sensor. The phase  $\alpha$  is obtained from the Fourier transform of this signal as described in Ref. 4. The surface profile of the object is given by  $r(x'') = (\lambda/8\pi)\alpha(x'')$ .

If the object is moved in parallel with the optical axis, the phase of  $U_o(x)$  or  $U_{1o}(x')$  changes uniformly in space with time. When the time-varying phase changes faster than the process of grating formation in the phase conjugator, the conjugator reflects a conjugate wave with the same uniform phase change.<sup>8</sup> Because no phase reversal for the uniform phase change of the object wave takes place, the phase changes of  $U_{1r}(x')$  and  $U_{1o}(x')$  are identical. So the interference pattern is not affected by the spatially uniform time-varying phase change of the object wave. The interferometer has a special feature that it is completely free of the disturbance in axial vibrations of objects.

### 2.2 Position of the Object Field in Image Space

In this interferometer, it is a key point to make the object field in the image space on the glass plate, and so the positions of glass plate and object surfaces are very important. If the glass plate is placed before or after the position where it should be kept, measurement errors will occur.

To find the relationship between the positions of the object fields in object and image spaces, the transformation of the object field with lenses  $L_3$  and  $L_4$  is shown in Fig. 2. The back focal point of lens  $L_3$  coincides with the front focal point of lens  $L_4$ . The  $f_3$  and  $f_4$  are the focal lengths of the two lenses, respectively. The object field on the object surface is located at the distance  $l_1$  from lens  $L_3$ . The object field in image space

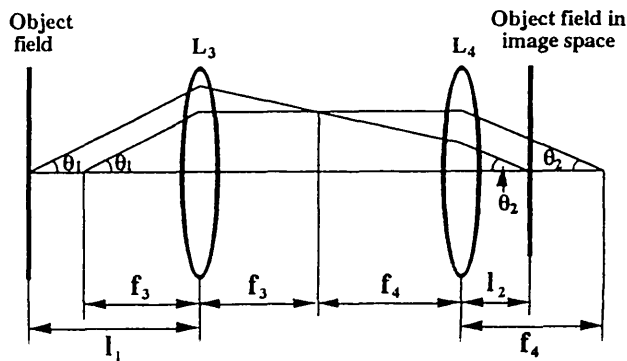


Fig. 2 Formation of the object field in image space.

is formed at the distance  $l_2$  from lens  $L_4$  on the surface of the glass plate. We consider two rays of light that propagate at an angle of  $\theta_1$  with the optical axis from the object field plane and front focal point of lens  $L_3$ , respectively. It is assumed that the lenses do not have any aberrations. These two rays reach in image space at an angle of  $\theta_2$  with the optical axis as shown in Fig. 2. The following relations are satisfied:

$$f_3 \tan\theta_1 = f_4 \tan\theta_2, \quad (8)$$

$$l_2 \tan\theta_2 = f_3 \tan\theta_1 - (f_4/f_3)(l_1 - f_3) \tan\theta_1. \quad (9)$$

From Eqs. (8) and (9), the position of the object field in image space is given by

$$l_2 = f_4 - (f_4/f_3)^2(l_1 - f_3). \quad (10)$$

When the distance  $l_1$  between the object and lens  $L_3$  and the distance  $l_2$  between the glass plate and lens  $L_4$  in Fig. 1 satisfy Eq. (10), the same phase distribution as the object surface will be formed on the glass plate with a magnification of  $f_4/f_3$ .

### 3 Measurements of 1-D Surface Profiles

#### 3.1 Experimental Setup

The experimental setup is shown in Fig. 1. The light source is an argon-ion laser operating in single longitudinal mode with an output power of 50 mW and wavelength  $\lambda = 514.5$  nm. The beam is expanded to a diameter of 5 mm with a microscopic objective lens  $L_1$  and lens  $L_2$ . Lenses  $L_3$  and  $L_4$  have the same focal length  $f_3 = f_4 = 100$  mm. The object is a diamond-turned aluminum disk, and the distance  $l_1$  is adjusted to  $f_3$ . To make the object field in image space on the glass plate, the distance  $l_2$  between the glass plate and lens  $L_4$  is adjusted to  $f_4$ . The surface of the glass plate coated with an antireflection layer faces lens  $L_6$ . The other surface reflects an object wave. The glass plate is attached to three PZTs. The object wave is phase modulated by vibrating the glass plate sinusoidally with PZTs. The beam transmitted through the glass plate is introduced to a photorefractive BaTiO<sub>3</sub> crystal with lens  $L_6$ . The diameter of the beam at the entrance to the crystal is  $\sim 2$  mm. The laser power incident on the crystal is  $\sim 5$  mW. The crystal has a dimension of  $5 \times 5 \times 5$  mm. The crystal axis is oriented horizontally at  $\sim 60$  deg to the optical axis of the incident beam. The interference pattern on the glass plate is imaged onto a 1-D CCD image sensor by lens  $L_5$ .

The pixel size of the CCD image sensor is  $9 \times 14 \mu\text{m}$  and its pixel interval is  $14 \mu\text{m}$ . The 28 elements of the CCD image sensor receive the interference signal and the remaining ones are covered with black paper. The magnification of the image is 2.5. Hence, the spatial interval of the measuring points is  $5.6 \mu\text{m}$  and the measuring range is  $156 \mu\text{m}$ . The surface profile is obtained through processing the interference signal detected by the CCD image sensor with the Fourier transform method.<sup>6</sup> The amplitudes of the output signal of the CCD image sensor decreases with the increment of the frequency of the sinusoidal phase modulation  $\omega/2\pi$ . We choose the modulation frequency to be 187 Hz to obtain the amplitudes large enough to carry out the experiments. In our experiments, the amplitude  $Z$  and phase  $\theta$  of the phase modulation are 2.58 rad and  $\pi$ , respectively. The CCD image sensor is operated

with a clock pulse of 1 MHz and a charge storage period of  $(2\pi/\omega_c)/8$ . The output of the CCD image sensor is analog-to-digital (A/D) converted and stored in a computer.

#### 3.2 Experimental Results

First, the diamond-turned aluminum disk was placed at the right position, which was determined by Eq. (9). Figure 3(a) shows the measured surface profile of the disk in which the tilt and the bias of the surface contained in the raw data have been eliminated. The surface profile has a periodic structure determined by the cutting pitch. The peak-to-peak roughness of the disk surface is  $\sim 100$  nm, and its period is  $\sim 50 \mu\text{m}$ . These values agree well with those of the surface profile measured with a Talystep instrument shown in Fig. 4. However, the fine profile of Fig. 3(a) is not completely the same as that of Fig. 4 because of different spatial intervals of measuring points, different measuring regions, and different measuring methods. The measurement of the same disk surface was repeated after an interval of a few minutes. The measured result is shown in Fig. 3(b). The measurement repeatability is below 0.5 nm.

Next, the effect of object's positions on the measurement was examined experimentally. The disk surface was moved backward and forward from the right position by 0.4 mm, that is, position errors of  $\Delta l = 0.4$  mm and  $\Delta l = -0.4$  mm were given. The measurement results are shown in Figs. 5(a) and 5(b), respectively. It is found that there is a little change in the measured cutting pitch while the peak-to-peak roughness obviously decreases with the increment of the position error. If we expect that the measurement error of the peak-

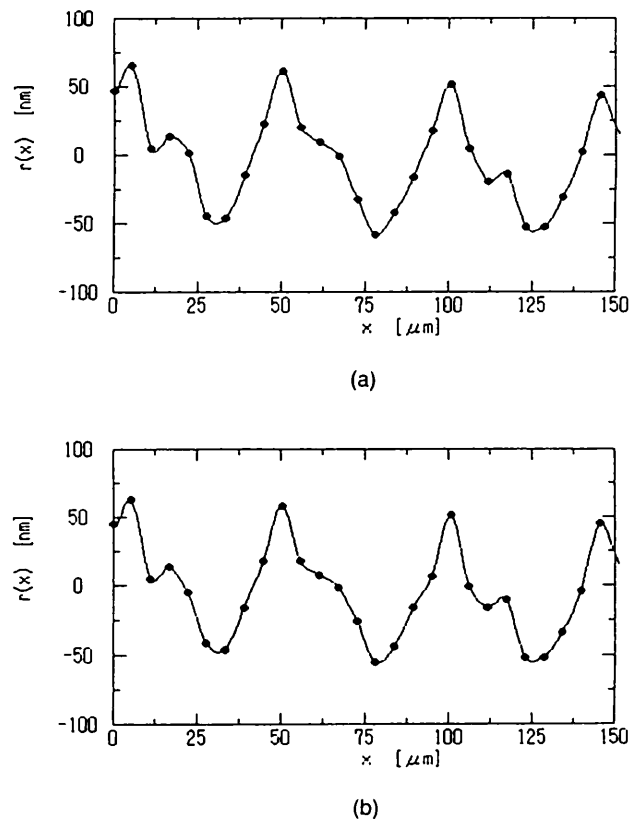


Fig. 3 (a) Surface profile of a diamond-turned aluminum disk. (b) The same surface disk measured after interval of a few minutes.

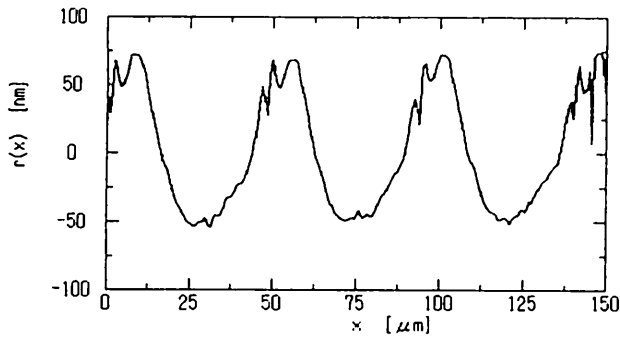


Fig. 4 Surface profile of a diamond-turned aluminum disk measured with a Talystep instrument.

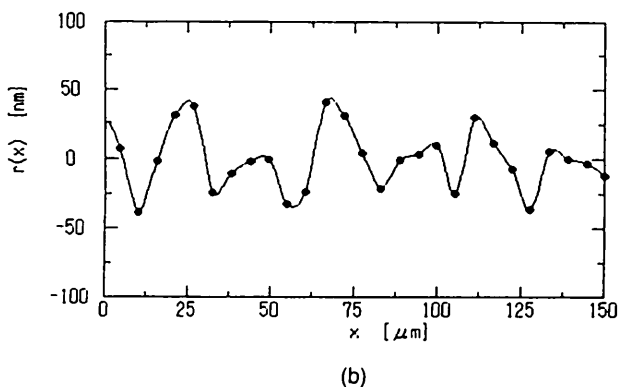
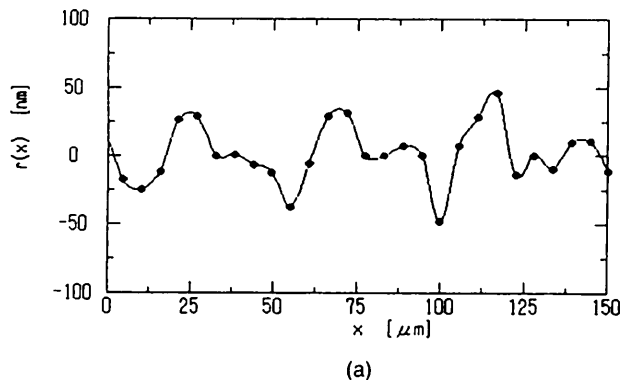


Fig. 5 Surface profiles of a diamond-turned aluminum disk measured with the position error (a)  $\Delta l = 0.4$  mm and (b)  $\Delta l = -0.4$  mm.

to-peak value is less than 20%, the position error must be less than 0.2 mm for the disk surface employed.

#### 4 Measurements of 2-D Surface Profiles

We constructed the interferometer shown in Fig. 1 and measured the surface profile of a diamond-turned aluminum disk. If this interferometer is used to test a large-diameter object, a large-size beamsplitter  $BS_1$  is required. To avoid this problem, we exchanged the positions of  $BS_1$  and lens  $L_2$  and developed the optical system shown in Fig. 6. Lenses  $L_1$  and  $L_2$  are arranged so that the object is illuminated by a collimated beam. Lenses  $L_2$  and  $L_3$  make a reduced object field in the image space on the glass plate. The dimensions of the glass plate are smaller than those of the object. The reduced scale of the dimensions is the ratios of the focal lengths of

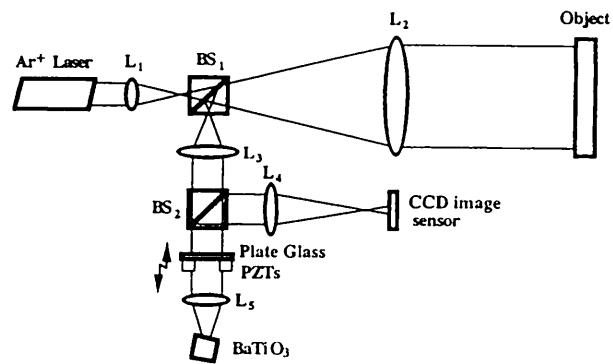


Fig. 6 SPM Fizeau interferometer using a phase conjugator for the surface profile measurement of large-diameter objects.

lenses  $L_3$  and  $L_2$ . The interference pattern between the object and phase conjugate waves on the glass plate is imaged on a 2-D CCD image sensor with lens  $L_4$ .

We measured the surface profile of a 20-mm-diam mirror. The microscopic objective  $L_1$  and lens  $L_2$  produce a collimated beam. The focal length of lens  $L_2$  is 500 mm. The object is kept at 200 mm from lens  $L_2$ . The focal length  $f_3$  of lens  $L_3$  is 70 mm. The distance  $l_2$  is determined by  $f_3 - (f_3/f_2)^2(L_1 - f_2)$  to be 76 mm. The beam through the glass plate is reduced to  $\sim 3$  mm in diameter. The image magnification from the glass plate surface to CCD image sensor plane was 0.19.

The mirror surface was imaged on the CCD image sensor with a magnification of 0.027. The horizontal and vertical pixel intervals of the CCD image sensor were 26.8 and 23.0  $\mu\text{m}$ , and the spatial intervals of the measuring points were 1.00 and 0.86 mm. The  $20 \times 20$  elements of the CCD image sensor were used to detect the interference signal, so the size of the measuring region was  $20.0 \times 17.2$  mm. The frequency of the sinusoidal phase modulation is 120 Hz. The amplitude and phase of the modulation were  $Z = 2.45$  and  $\theta = 56$  deg, respectively. The clock pulse frequency of the CCD image sensor was  $\sim 8$  MHz, and its storage period was  $(2\pi/\omega_c)/4$ . The outputs of the CCD image sensor were sampled by an A/D converter to be processed in a computer. The surface profiles were obtained through the integrating-bucket method.<sup>7</sup>

Figure 7 shows the measured surface profile of the mirror. The tilt of the surface was subtracted and the effect of the noise was reduced to a large extent by averaging nine detected-value sets. The root mean square (rms) and the peak-valley (P-V) values of the measured surface are 25.6 and 126 nm, respectively. The measurement repeatability was  $\sim 1.8$  nm.

To examine the effect of object's position on the measurement, we measured the same mirror surface with different position errors. Figure 8 shows the measurement result with the position error  $\Delta l = 5$  mm. The surface profile is almost the same as Fig. 7. The rms and P-V values are 23.0 and 120 nm, respectively. Compared with the diamond-turned aluminum disk, the effect of position errors is quite small. This is because the surface profile of the mirror has a much longer period than that of the diamond-turned aluminum disk, and the maximum diffraction angle of light beams from the

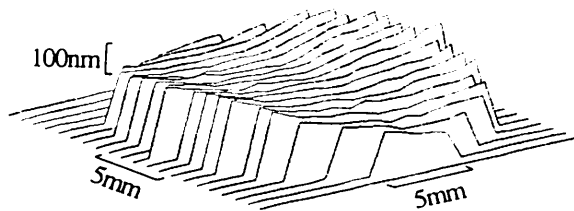


Fig. 7 Measured surface profile of a mirror.

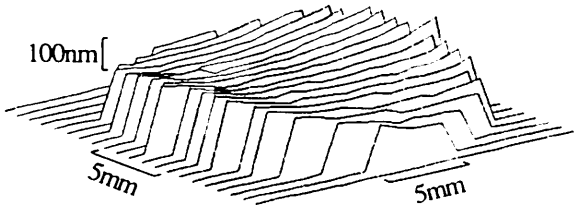


Fig. 8 Surface profile of a mirror measured with the position error  $\Delta l = 5$  mm.

disk surface is several hundred times as large as that from the mirror surface.

## 5 Conclusions

We have demonstrated a sinusoidal phase-modulating Fizeau interferometer with a self-pumped conjugator for surface profile measurements. The object field is formed on the surface of the glass plate where the object wave interferes with its phase conjugate wave. The positions of the object surface and the surface of the glass plate are important in the interferometer. The effects of the position error were examined experimentally. In the interferometer, the size of the glass plate need not be larger than or equal to that of the object. The small-size glass plate easily provides an accurate phase modulation for measuring large-diameter objects. It was made clear through the surface profile measurements of a diamond-turned aluminum disk and mirror that the interferometer is useful for the highly accurate measurements.

Because this interferometer is self-referencing, the effects of spatially uniform vibrations of object surfaces are eliminated. Furthermore, there is a high possibility that spatially nonuniform phase change of the object wave is not reversed on the self-pumped phase conjugation if the phase change is small. So the self-referencing interferometer could be free of any kinds of vibrations of the objects. The characteristics of the self-pumped phase conjugator for the spatial phase change of the object wave are now under study.

## References

1. J. Feinberg, "Interferometer with a self-pumped phase-conjugating mirror," *Opt. Lett.* **8**, 569-571 (1983).
2. R. P. Shukla, M. Dokhanian, P. Venkateswarlu, and M. C. George, "Phase conjugate Twyman-Green interferometer for testing conicoidal surfaces," *Proc. SPIE* **1332**, 274-286 (1990).
3. E. R. Parshall and M. Cronin-Golomb, "Phase-conjugate interferometric analysis of thin films," *Appl. Opt.* **30**, 5090-5093 (1991).
4. R. P. Shukla, M. Dokhanian, M. C. George, and P. Venkateswarlu, "Laser beam collimation using a phase conjugate Twyman-Green interferometer," *Opt. Eng.* **30**, 386-390 (1991).
5. D. J. Gauthier and R. W. Boyd, "Phase-conjugate Fizeau interferometer," *Opt. Lett.* **14**, 323-325 (1989).
6. O. Sasaki and H. Okazaki, "Sinusoidal phase modulating interferometry for surface profile measurement," *Appl. Opt.* **25**, 3137-3140 (1986).
7. O. Sasaki, H. Okazaki, and M. Sakai, "Sinusoidal phase modulating interferometer using integrating-bucket method," *Appl. Opt.* **26**, 1089-1093 (1987).
8. Y. Tomita, R. Yahalom, and A. Yariv, "Phase shift and cross talk of a self-pumped phase-conjugate mirror," *Opt. Commun.* **73**, 413-418 (1989).



**Xiangzhao Wang** received the BE degree in electrical engineering from Dalian University of Science and Technology, China, in 1982 and the ME degree in electrical engineering from Niigata University in 1992. He is currently working toward a PhD in the Graduate School of Science and Technology at Niigata University. His research interests include optical measuring systems, applications of phase conjugate optics, and optical information processing.

**Osami Sasaki:** Biography and photograph appear with the paper "Real-time two-dimensional surface profile measurement in a sinusoidal phase-modulating laser diode interferometer" in this issue.



**Yuuichi Takebayashi** received the BE degree in electrical engineering from Niigata University in 1993. He has been involved in surface profile measurements with interferometers. He is a graduate student at Niigata University.

**Takamasa Suzuki:** Biography and photograph appear with the paper "Real-time two-dimensional surface profile measurement in a sinusoidal phase-modulating laser diode interferometer" in this issue.

**Takeo Maruyama:** Biography and photograph appear with the paper "Real-time two-dimensional surface profile measurement in a sinusoidal phase-modulating laser diode interferometer" in this issue.